Water Research 247 (2023) 120809

Contents lists available at ScienceDirect

Water Research

journal homepage: www.elsevier.com/locate/watres

The distinct phases of fresh-seawater mixing intricately regulate the nitrogen transformation processes in a high run-off estuary: Insight from multi-isotopes and microbial function analysis

Yunchao Wu [a,b,c], Jinlong Li [a,b,d], Xia Zhang [a,b,c], Zhijian Jiang [a,b,c,d], Songlin Liu [a,b,c], Jia Yang [a,b,c], Xiaoping Huang [a,b,c,d,*]

[a] Key Laboratory of Tropical Marine Bio-resources and Ecology, South China Sea Institute of Oceanology, Chinese Academy of Sciences, Guangzhou 510301, China
[b] Southern Marine Science and Engineering Guangdong Laboratory (Guangzhou), Guangzhou 511458, China
[c] Guangdong Provincial Key Laboratory of Applied Marine Biology, Guangzhou, 511458, China
[d] University of Chinese Academy of Sciences, Beijing 100049, China

ARTICLE INFO

Keywords:
Nitrogen transformation
Multiple isotopes
Mixing process
Microbial function
Pearl River Estuary

ABSTRACT

Excessive anthropogenic nitrogen inputs lead to the accumulation of nitrogen, and significantly impact the nitrogen transformation processes in estuaries. However, the governing of nitrogen during its transport from terrestrial to estuary under the influence of diverse human activities and hydrodynamic environments, particularly in the fresh-seawater mixing zone, remains insufficient researched and lack of basis. To address this gap, we employed multi-isotopes, including δ^{15}N-NO_3^-, δ^{18}O-NO_3^-, δ^{15}N-NH_4^+, and δ^{15}N-PN, as well as microbial function analysis, to investigate the nitrogen transformation processes in the Pearl River Estuary (PRE), a highly anthropogenic and terrestrial estuary. Principle component analysis (PCA) confirmed that the PRE could clearly partitioned into three zone, e.g., terrestrial area (T zone), mixing area (M zone) and seawater area (S zone), in terms of nitrogen transportation and transformation processes. The δ^{15}N-NO_3^- (3.38±0.60‰) and δ^{18}O-NO_3^- (6.35±2.45‰) results in the inner estuary (T area) indicate that NO_3^-attributed to the domestic sewage and groundwater discharge in the river outlets lead to a higher nitrification rate in the outlets of the Pearl River than in the reaching and seawater intrusion areas, although nitrate is rapidly diluted by seawater after entering the estuary. The transformation of nitrogen in the T zone was under significant nitrogen fixation (0.61 ± 0.22 %) and nitrification processes (0.0043 ± 0.0032 %) (presumably driven by *Exiguobacterium sp.* (14.1 %) and *Cyanobium_PCC-6307* (8.1 %)). In contrast, relatively low δ^{15}N-NO_3^- (6.83 ± 1.24‰) and high δ^{18}O-NO_3^- (22.13 ±6.01‰) imply that atmospheric deposition has increased its contribution to seawater nitrate and denitrification (0.53±0.13 %) was enhanced by phytoplankton/bacterial (such as *Psychrobacter sp.* and *Rhodococcus*) in the S zone. The assimilation of NH_4 results from the ammonification of NO_3^- reduces δ^{15}N-NH_4^+ (5.36 ± 1.49‰) and is then absorbed by particulate nitrogen (PN). The retention of nitrogen when fresh-seawater mixing enhances the elevation of δ^{15}N-NH_4^+ (8.19 ± 2.19‰) and assimilation of NH_4^+, leading to an increase in PN and δ^{15}N-PN (6.91 ± 1.52‰) from biological biomass (mainly *Psychrobacter sp.* and *Rhodococcus*). The results of this research demonstrate a clear and comprehensive characterization of the nitrogen transformation process in an anthropogenic dominated estuary, highlighting its importance for regulating the nitrogen dissipation in the fresh-seawater mixing process in estuarine ecosystems.

1. Introduction

Estuaries are situated at the interface between land and ocean, and act as a major link between terrestrial and marine nutrient cycles (Gruber, 2008; Wong et al., 2018). Rapid increases in population and urbanization have dramatically raised dissolved inorganic nitrogen (DIN) loading in estuaries, resulting in water quality deterioration, habitat alterations, and biodiversity decline (Diaz and Rosenberg, 2008; Sinha et al., 2017). Excessive anthropogenic nitrogen input would alter the nitrogen transformation processes and further accelerate nitrate or

* Corresponding author at: South China Sea Institute of Oceanology, Chinese Academy of Sciences, Guangzhou 510301, China.
E-mail address: xphuang@scsio.ac.cn (X. Huang).

https://doi.org/10.1016/j.watres.2023.120809
Received 8 June 2023; Received in revised form 12 September 2023; Accepted 28 October 2023
Available online 28 October 2023

ammonium accumulation (Schlesinger, 2009), though only a small proportion of DIN from rivers discharge can be directly assimilated/adsorbed by phytoplankton in estuarine waters (Souza et al., 2021). In addition, a sizable portion of DIN transported to estuaries undergoes various biogeochemical transformations, such as nitrification and denitrification, before being assimilated by phytoplankton. These transformations are particularly pronounced in the freshwater and seawater mixing zones, where the complexity and intensity of bio-transformations are high (Hodoki et al., 2013). Despite the importance of these transformations, there is still a dearth of direct evidence that can shed light on the mechanisms of nitrogen transformation in estuaries, especially in those highly hydrodynamic zones under fresh-seawater mixing processes. As a result, the fate of nutrients with high bioactivity, and the mechanisms by which elevated nitrogen (including nitrate (NO_3^-), ammonium (NH_4^+) and particulate nitrogen (PN)) accumulates and transformed in these areas, remain poorly understood (Seitzinger et al., 2002).

Stable isotopes of nitrogen (e.g., $\delta^{15}N\text{-}NO_3^-$, $\delta^{18}O\text{-}NO_3^-$, $\delta^{15}N\text{-}NH_4^+$, and $\delta^{15}N$-PN are useful tools in resolving the sources of nitrogen within the scope of their respective forms, as the various nitrogen sources have distinct isotopic signals (Jiang et al., 2021; Xuan et al., 2020; Ye et al., 2022; York et al., 2007). They are also sensitive compass in predicting the transformation processes (e.g., assimilation, nitrification, denitrification, and ammonification) along the transportation of nitrogen along the upstream to the downstream/estuary, especially when fresh-seawater mixed (Nikolenko et al., 2018; Wong et al., 2018; Xuan et al., 2020). Nitrification is a typical nitrate source process, which could be traced by depleted $\delta^{15}N\text{-}NO_3^-$ values from anthropogenic and terrestrial sources and enriched $\delta^{15}N\text{-}NH_4^+$ values due to the preferential incorporation of the lighter isotopes into the production of NO_3^- (Archana et al., 2018; Denk et al., 2017). Assimilation is a temporary sink process of nitrogen and could exchange nitrogen with sediment, which results in the $\delta^{15}N$ decrease due to the produced organic nitrogen and leads to the $\delta^{15}N$ and $\delta^{18}O$ values increase while the remaining $\delta^{15}N$ and $\delta^{18}O$ of nitrate keeping close to 1:1 line during NO_3^- uptake by phytoplankton (Granger et al., 2004). The denitrification is a permanent sink process of nitrate, which leads to the simultaneous increase of residual $\delta^{15}N\text{-}NO_3^-$ and $\delta^{18}O\text{-}NO_3^-$ (Denk et al., 2017; Nikolenko et al., 2018), and the ratios of the increase of the $\delta^{15}N$ and $\delta^{18}O$ values of the remaining nitrate are assumed to be close to 1.5:1 or even 2:1 (Kendall et al., 2001). Currently, there exists a significant knowledge gap concerning the intricate transportation and transformation processes involving nitrogen, particularly the relationships among various nitrogen forms within biological and microbial interactions occurring. This is particularly crucial in the mixing zone, where freshwater meets seawater and is diluted by it in the turbidity maximum zone (Keats et al., 2004; Lin et al., 2022).

Microorganisms play a pivotal role as crucial biological agents driving nitrogen transformation within estuarine aquatic ecosystems. (Adyasari et al., 2020; Zhu et al., 2019). Microorganisms can colonize the surface of particulate nitrogen in the form of Lifshitz-van der Waals attraction for growth and maturation (Zhang et al., 2022). The probability of particulate matter with available nitrogen in the water determines the microbial community composition and nitrogen transformation processes (Karthäuser et al., 2021). Estuaries with high flow volume water input were accompanied by high resuspended particulate fluxes and high nitrogen inputs, which elevated this probability and led to marked spatial heterogeneity in the formation of microbial communities, and therefore impact the nitrogen transformation between different nitrogen forms (Adyasari et al., 2020; McLaughlin et al., 2017). However, the relationship between microorganisms and nitrogen transformation in estuarine regions remains unclear, particularly in terms of utilizing isotopic composition and microbial processes to characterize the transportation and transformation of nitrogen species. As such, straightforward evidence has yet to be obtained (Zhang et al., 2022; Zhu et al., 2019).

To date, concentrations, sources and flux of nitrogen originating from riverine freshwater (Jiang et al., 2021), groundwater (Nikolenko et al., 2018), and atmospheric precipitation (Wu et al., 2018) in estuaries have been carried out in previous studies. Nevertheless, the intricate hydrodynamic conditions within estuaries underscore a multifaceted nitrogen source and sink mechanism, wherein the translocation and transformation of nitrogen components during the pronounced confluence of fresh-seawater remain elusive. Therefore, it is urgent to explore the nitrogen translocation and transformation processes in the coastal fresh-seawater mixing system, which hides more complex and diverse nitrogen transformation processes (Bruesewitz et al., 2013; Loken et al., 2016), particularly the role of marine microorganisms assimilation in the transformation process of nitrogen between dissolved and particulate forms, beyond physical adsorption, remains uncertain (Karthäuser et al., 2021; Seitzinger et al., 2002). To gain a deeper comprehension of nutrient accumulation and assimilation in estuaries with substantial terrestrial input, it is imperative to scrutinize the transformations of nitrogen, especially during the intersection of fresh-seawater exchange (Dähnke et al., 2008b; Swart et al., 2014).Therefore, our study endeavors to elucidate the fate of nitrogen within estuaries subjected to varying seasons and characterized by significant differences in hydrodynamics. We employ isotopes and assess microbial functions to gain insights into the nitrogen transformation processes in estuaries influenced by terrestrial and anthropogenic inputs, with a particular emphasis on understanding these processes within the fresh-seawater mixing zone. The results of this study will helps in formulating effective management strategies for estuarine ecosystems, which are of both ecological and economic importance.

2. Sampling and methods

2.1. Study area description

This study was conducted in the Pearl River Estuary (PRE) (21°27′–22°48′N, 113°00′–114°30′E) (Fig. 1), South China. The PRE region is a highly developed and densely populated area in China. In the past decade, the cropland area in PRE delta has experienced a reduction, while the expanse of construction land has undergone a substantial increase (Fig. S1) (Wang et al., 2021), resulting in a significant anthropogenic nitrogen load from sources such as agriculture, aquaculture, and domestic/industrial sewage. During the rainy seasons (April to September), which accounts for almost 70 % of the annual runoff in the PRE, the substantial freshwater discharge in the region leads to the formation of a freshwater plume, resulting in the extensive dispersion of diluted water throughout the estuary. In contrast, during winter, when freshwater discharge is low and tidal currents are more dominant, the separation of freshwater and saline water becomes more distinct.

2.2. Sample collection and analysis

2.2.1. Sample col. lections and environmental parameters

This study involved four research cruises conducted in July 2019, January 2020, August 2020, and January 2021, as depicted in Fig. 1. The July 2019 and August 2020 cruises were conducted during the summer season (July to September) when there was strong runoff input (referred to as summer), while the January 2020 and January 2021 cruises were conducted during the winter season (January to March, referred to as winter). The four cruises were strategically scheduled during the midpoints of the summer and winter seasons, and a total of 198 water samples and CTD profiles were collected, covering a salinity range of 0 to 35 and representing the various water types typically encountered in river-influenced ocean margins, ranging from riverine to oligotrophic marine.

Environmental parameters, including salinity, temperature (℃), pH, dissolved oxygen (DO, mg/L), and chlorophyll a (Chla, μg/L), were measured using a RBRconcerto^3 (Canada) detector. Seawater samples

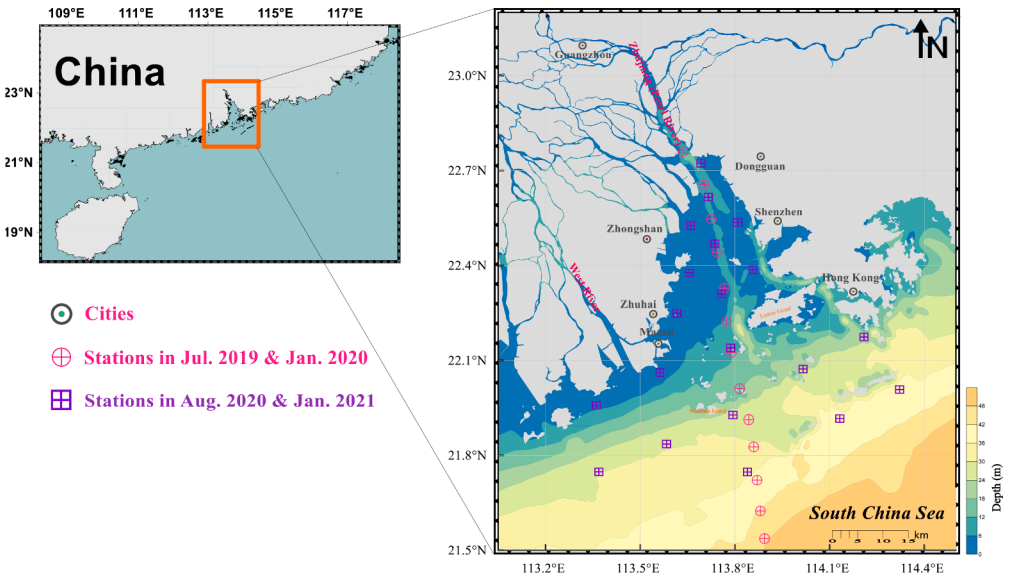

Fig. 1. Sampling sites and cruises description. The water column layers are collected according to the depth, and surface and bottom layers were collected at the station depth of less than 5m, and three water layers (surface, middle, and bottom layer) samples were collected at the station depth between 5-10m; 0, 5, 10 and bottom layer water samples were collected when the station depth 20-30m; 0, 10, 20, and bottom water samples were collected when station depth higher than 30m.

were collected using a 5 L Niskin (General Oceanics, USA) bottle and vacuum-filtered using pre-combusted (450 ℃, 4 h) glass-fiber filters (Whatman GF/F, 47 mm, 0.7 μm). Subsamples were preserved for nutrient and isotope analysis, and all samples were stored in pre-cleaned polyethylene bottles at -20℃ until analysis.

POC and PN samples were vacuum-filtered using pre-combusted (450 ℃, 4 h) glass-fiber filters (Whatman GF/F, 25 mm in diameter, 0.7 μm in pore size), and were acidified with 5 ml 1M HCl (Analytically pure, Merck, German) to remove inorganic carbon for 24 h and washed with distilled water.

2.2.2. *Dissolved inorganic nitrogen species analysis*

Nutrient species (including NH_4^+, NO_3^- and NO_2^-) were analyzed using an AA3 auto continuous-flow analyzer following standard procedures for seawater nutrient analysis, with detection limit at 0.03 μmol/L, 0.05 μmol/L, and 0.03 μmol/L, respectively. DIN was calculated as the sum of NH_4^+, NO_3^-, and NO_2^-. TDN were analyzed via high-temperature catalytic oxidation using a TOC-L automatic analyzer (TOC-V_{CPH}-NML), with an accuracy of 1.2 % and 2.3 %, respectively.

POC and PN were analyzed using an elemental analyzer at 980 ℃ to calculate the organic fractions of carbon and nitrogen (Flash EA 3000 Thermo Scientific, Milan, Italy) with L-Cystine as the reference standard. The accuracies for POC and PN were better than 99 % and 97.5 %, respectively.

2.2.3. *Isotopic analysis*

Nitrogen and oxygen isotope analysis were measured by the denitrifier method (Sigman et al., 2001). A batch of denitrifier strain *Pseudomonas aureofaciens* (ATCC 13985) was cultured to denitrify nitrate and nitrite to N_2O. Subsequently, the dual isotopes of N_2O gas were determined online using GasBench II coupled with a continuous flow isotope ratio mass spectrometer (IRMS, Thermo Finnigan DELTA$_{plus}$). The $\delta^{15}N$ and $\delta^{18}O$ values were corrected for drift, oxygen isotopic exchange was eliminated by international nitrate isotope standards USGS32, USGS34, USGS35 (Böhlke et al., 2003).

The determination of $\delta^{15}N$-NH_4^+ values was conducted using a diffusion method, as described in the procedures established by Chen and Dittert (2008). A 5-liter sample was collected from each site in a high-density polyethylene diffusion bottle that had been pre-cleaned. To assess the isotopic fractionation during the diffusion process, three control samples were also prepared. These consisted of ammonium sulfate solutions with NH_4^+ concentrations that were approximately equal to those found in the seawater, and with $\delta^{15}N$ values of -2.37‰ ± 0.03‰. To make ammonia traps, sulfuric acid-impregnated fibers (GF/D, Whatman) were sandwiched between two Teflon membranes (Millipore LCWP 02500). The diffusion bottles were then tightly sealed and incubated at 40 °C for two weeks, after which 200 g of sodium chloride, 15 g of magnesium oxide, and the ammonia trap were added to each bottle. The GF/D fibers were then dried and the $\delta^{15}N$-NH_4^+ values were determined. $\delta^{15}N$-NO_3^-, $\delta^{18}O$-NO_3^- and $\delta^{15}N$-NH_4^+ were analyzed at the Analytical and Testing Center of the Third Institute of Oceanography, Ministry of Natural Resources, China, duly authorized as the IAEA Collaborating Center for marine environmental isotope analysis (2022–2026).

The $\delta^{13}C$-POC and $\delta^{15}N$-PN isotope samples were analyzed by a continuous-flow isotope-ratio mass spectrometer (Delta V Advantage, Thermo Fisher Scientific). The reference standards for $\delta^{13}C$ and $\delta^{15}N$ were Pee Dee Belemnite standard. The accuracies of the isotopic analysis were better than ±0.2‰ and ± 0.3‰ for $\delta^{13}C$ and $\delta^{15}N$, respectively. $\delta^{13}C$-POC and $\delta^{15}N$-PN were analyzed in the Equipment Public Service Center, South China Sea Institute of Oceanology.

2.2.4. *Bacterial community and function analysis*

An approximately 1 L sample of surface seawater was collected at each station during the July 2020 cruise (n=2; 1 L per replicate). The samples were pre-filtered through 1.2 μm poly-carbonate filters to remove large and suspended particles, followed by filtration through 0.22 μm filters (Millipore Corp., Bedford, MA, USA) to capture bacteria. The bacteria collected on the 0.22 μm filter membranes were preserved in 0.8 mL extraction buffer (500 mM NaCl, 50 mM Tris-HCl, 40 mM EDTA, and 0.75 M sucrose; pH 8) at -20 °C. The extraction buffer contained a high concentration of sucrose, which prevents immediate osmotic lysis of the bacteria and helps to maintain DNA integrity, as confirmed by previous studies. Bacterial community analysis was conducted using 16S rRNA gene amplicon sequencing, while shotgun sequencing (Whole Genome Sequencing) was employed to map the metabolic potential of the microbial communities. We predicted the bacterial functional profiles of core microbiota in *E. ulmoides* bark using Functional Annotation of Prokaryotic Taxa (FAPROTAX). FAPROTAX is more suitable for predicting the biogeochemical cycle of samples

(especially the cycle of carbon, hydrogen, nitrogen, phosphorus, sulfur, and other elements).

2.3. Data process

The deviation of the isotopes from the expected conservative mixing values to explore the nitrogen transformation process from the dissolved (Sigman et al., 2005) and particle phase of nitrogen.

$$\Delta(15,18) = \Delta\delta^{15}N - \left({}^{15}\varepsilon/{}^{18}\varepsilon\right) \times \Delta\delta^{18}O$$

where $\Delta\delta^{15}$N and $\Delta\delta^{18}$O are the differences between the observed and theoretical isotope values for conservative mixing, and ${}^{15}\varepsilon/{}^{18}\varepsilon$ is the isotope enrichment ratio during NO_3^- assimilation or denitrification (Dähnke et al., 2008b). A slope of one is typical for marine ecosystems. A Δ(15, 18) value close to 0 suggests denitrification and/or assimilation as the major NO_3^- transformation process, while a negative Δ(15, 18) value suggests concurrent NO_3^- removal (denitrification and/or assimilation) and generation (N fixation and/or nitrification) (Sigman et al., 2005).

Data in summer and winter seasons, and different regions were first evaluated to determine if the assumptions of homogeneity and normality were met. The difference in isotope composition in dry and wet seasons was assessed with independent sample *t*-tests. The relationships between different parameters and isotopes were examined using regression analyses, with a significance level of $p<0.05$ being considered significant. The predictive strength of environmental variables and nutrient concentrations on the overall isotopes of the water samples collected in both seasons was explored using partial least squares regression (PLSR) conducted with the SIMCA 14.1 software (Umetrics). The PLSR model was chosen due to its ability to handle the collinearity of multiple variables and identify an optimal set of orthogonal principal components from the dataset, thereby maximizing the explanation of variability between the predictor and response variables. Statistical analyses, including mean values and differences, were performed with IBM SPSS 22.0 software. Environmental parameter, nutrient concentrations, and isotopes were normalized and carried out by principal component analysis (PCA) using OriginLab Pro 2022. The interaction between the physicochemical characteristics, isotopes and microbial biomass was normalized and investigated using relevance redundancy analysis (RDA) using OriginLab Pro 2022.

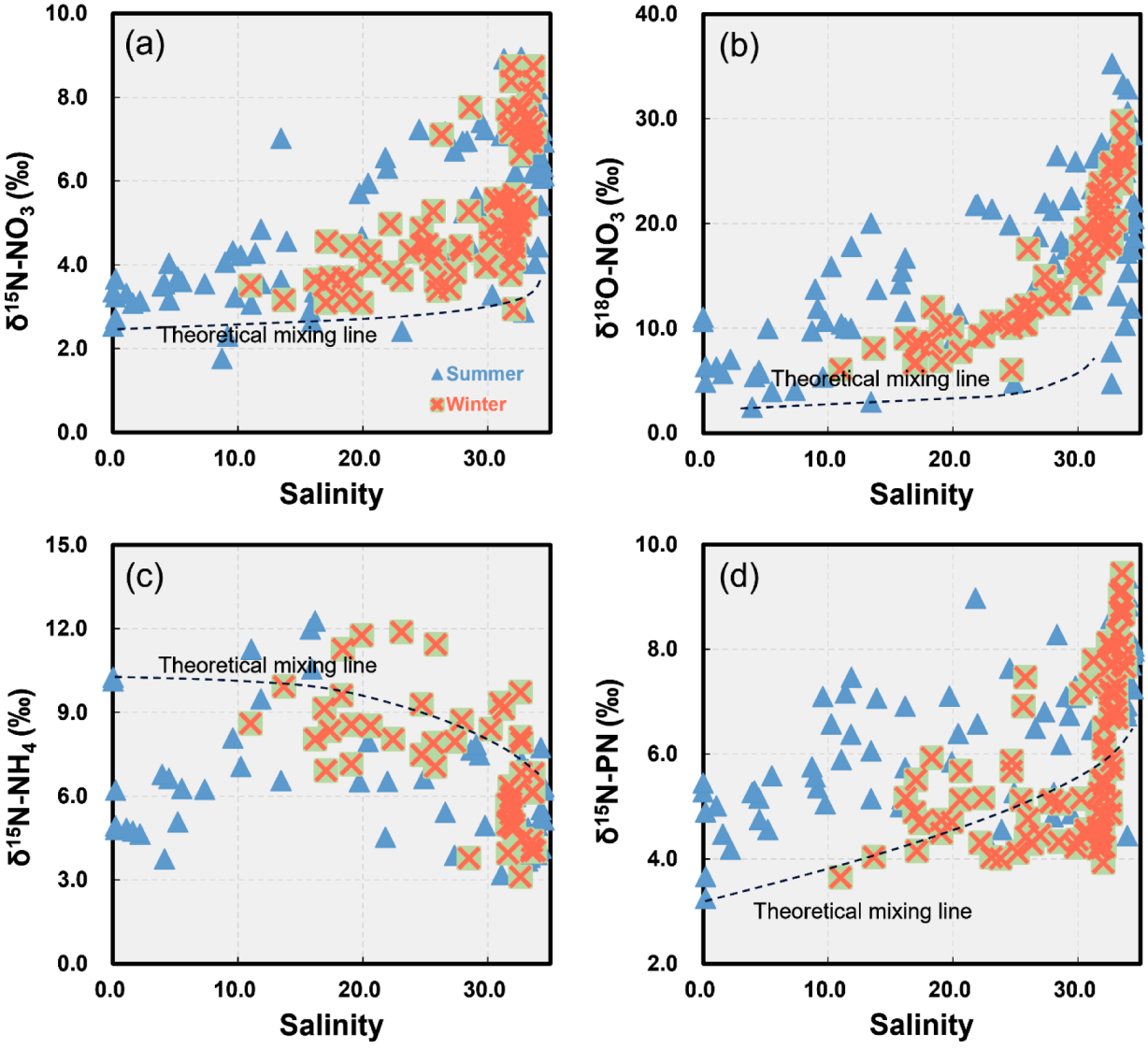

Fig. 2. Isotopic signatures (δ^{15}N-NO_3^-, δ^{18}O-NO_3^-, δ^{15}N-NH_4^+, and δ^{15}N-PN) along salinity gradient in different seasons. The blue triangles are data in the summer seasons, while the organic ones are data in the winter seasons.

3. Results

3.1. Isotopic signature of NO_3^-, NH_4^+, and PN

The isotopic signature of δ^{15}N- NO_3^-, δ^{18}O- NO_3^-, δ^{15}N-NH_4^+, and δ^{15}N-PN varied clearly along the salinity gradient. As shown in Fig. 2(a) and (b), the δ^{15}N-NO_3^- values ranged from 1.77‰ to 8.95‰ with a mean value of 5.19 ± 1.85‰ in the summer seasons, while it has a narrow range from 2.94‰ to 9.00‰ with a mean value of 5.50 ± 1.61‰ in winter seasons. However, no significant differences were found between seasons ($p = 0.31$). The δ^{15}N-NO_3^- values of all the seasons increased along the salinity gradient, typically exponentially increased in the winter season, due to the reduced impact of runoff input compared to that in summer (Fig. S3). The δ^{18}O-NO_3^- values trended to increase from the low salinity (2.47‰, upper stream) to the seaward in the outer of the PRE estuary (35.28‰, high salinity). It ranged from 2.47 to 35.28‰ with a mean value of 15.79 ± 8.23‰ in summer, whereas from 6.08 to 27.79‰ with a mean value of 16.01 ± 6.53 ‰ in winter. Significant differences of δ^{18}O-NO_3^- values between summer and winter seasons were observed ($p = 0.02$), indicating notable seasonal variations.

The overall δ^{15}N-NH_4^+ values displayed a range of +3.68‰ to +12.23‰ with an average of 6.29 ± 2.14‰ in the summer seasons, and a range of 3.12‰ to 11.88‰ with an average of 7.10 ± 2.22‰ in the winter seasons (Fig. S4). The seasonal variation of the δ^{15}N-NH_4^+ was found to be statistically significant ($p < 0.01$, Fig. 2(c)) with the average value being higher in the winter seasons compared to the summer seasons. The overall δ^{15}N-PN values ranged from +3.24‰ to +9.36‰ with an average of 6.51 ± 1.41‰ in the wet season and ranged from +3.65‰ to +9.45‰ with an average of 5.84 ± 1.54‰ in the dry season. Specially, the variations of the δ^{15}N-PN between seasons was not significant ($p = 0.19$, Fig. 2(d)).

3.2. Spatial discrimination and drivers

The impact of terrestrial inputs affects the annual salinity changes. To verify the reliability of multiple isotopes, we utilized PCA analysis to partition the estuary into three distinct regions, namely the terrestrial area (T area), mixing area (M area), and seawater area (S area) (see detailed sites information in Figure S9 in the supplementary material). PCA results based on the environmental variables, nutrient concentration and multiple isotopes (all parameters are normalized) showed that PC1 explained 44.94 % of these variables, which is referred as the NO_3^- transformation process dominated by the salinity (terrestrial input). PC2 accounts for 13.58 % of the variance and is associated with the biochemical (DO, Chla, and T dominated) process, as evidenced by the opposing trends observed in POC/PN and NH4+ levels. Loadings on PC2 suggest a decoupling or mutual transformation between NH_4^+ and POC/PN. On the other hand, based on the distribution of the isotopes and environmental variables of all the water layers, we identified three distinct zones, namely the terrestrial input area (orange ellipse), the mixing area (green ellipse), and the seawater area (purple ellipse) (95 percent based confidence) (Fig. 3). The reliability of the three-region partitioning is confirmed by the successful validation of isotopic data using the partial least squares regression (PLSR) model (see in the supplementary material and Fig. S7).

3.3. Characteristics of bacterial community structure related to inorganic nitrogen

The microbial community in different water layers revealed significant inconsistencies among dominant species in relation to salinity (Fig. 4(a)). For instance, *Psychrobacter sp.* and *Exiguobacterium sp.* were found to dominate in the mixing area, which is characterized by a complex hydrological environment and nutrient transformation zones. *Exiguobacterium sp.* and *Cyanobium_PCC-6307* accounted for the highest contribution (14.1 % and 8.1 %, respectively) in the T zone, despite being the dominant species in the freshwater receiving area. Conversely, *Psychrobacter sp.* dominated the S zone where all samples exhibited salinity levels exceeding 30, indicating its prevalence in a seawater-controlled region.

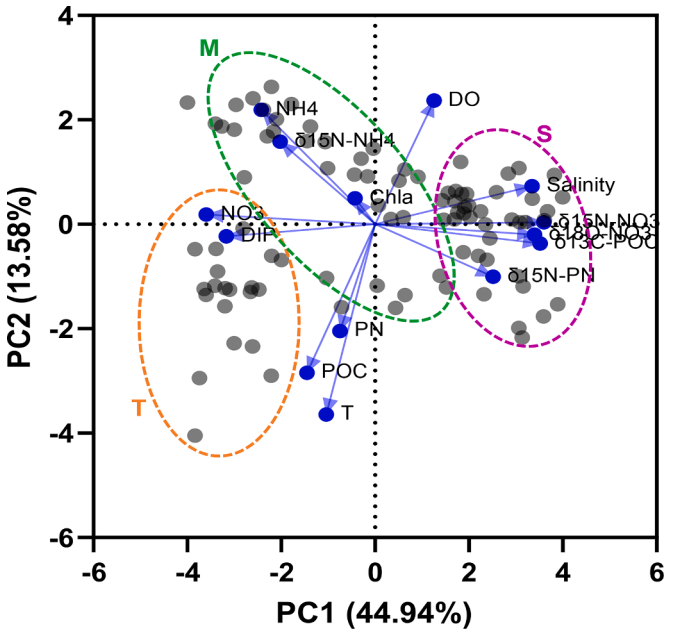

Fig. 3. PCA analysis of environmental variables, nutrient concentrations, and multiple stable isotopes (δ^{15}N-NO_3^-, δ^{18}O-NO_3^-, δ^{15}N-NH_4^+, and δ^{15}N-PN) indicating a region-based distribution pattern in PRE (95 percent based confidence). The left ellipse (orange one) includes stations in the upstream of PRE (the terrestrial influenced area, T), the green ellipse includes those stations in the mixing area (S), and the purple ellipse correspond to the sampling stations in the sea influenced sites (S). Specific sample classification please see in Fig. S9 of the supplementary material.

The FAPROTAX function prediction results revealed significant differences in the proportion of nitrogen fixation among the T zones (0.61 ± 0.22 %), M zone (0.082 ± 0.036 %), and S zones (0.016 ± 0.013 %) (Fig. 4(b)). Furthermore, nitrification was found to be higher rates in the T zone (0.0043±0.0032 %), though the rate of nitrification is relatively low compared to other processes. As for denitrification and ammonification, both processes appeared to be more prominent in the S zones (0.53 ±0.13 % and 0.0080 ± 0.0072 %, respectively), although statistical significance was not established (Fig. 4(b)).

The results from the RDA analysis showed notable variations among different water layer, with RDA1 (60.03 %) and RDA2 (30.09 %) explaining 90.12 % of all the variables (Fig. 5). RDA1 was indicative of a nitrate-dominated axis, with the sites distributed from right to left. Meanwhile, RDA2 was linked to a microbial/nitrate assimilation-derived axis, as evidenced by the distinct deviation of dominant microbial species from top to bottom, effectively segregating terrestrial and seawater-dominated species. *Psychrobacter sp.* was found to be well-correlated with δ^{15}N-NO_3^- and δ^{18}O-NO_3^-, and deviated from terrestrial sites characterized by higher nitrate loadings. δ^{15}N-NO_3^- exhibited a significant positive correlation with two marine-derived microbial species, namely, *Rhodococcus* and *Rhizobiaceae*. Furthermore, *Synechococcus_CC9902* was predominant in regions with high salinity sites, while in fresh-seawater mixing areas, *Cyanobium_PCC6307* and *Psychrobacter* were well-correlated with δ^{15}N-NO_3^-.

4. Discussion

4.1. Sources and fate of nitrate during fresh-seawater interaction

The concentration of nitrate was significantly higher than that of

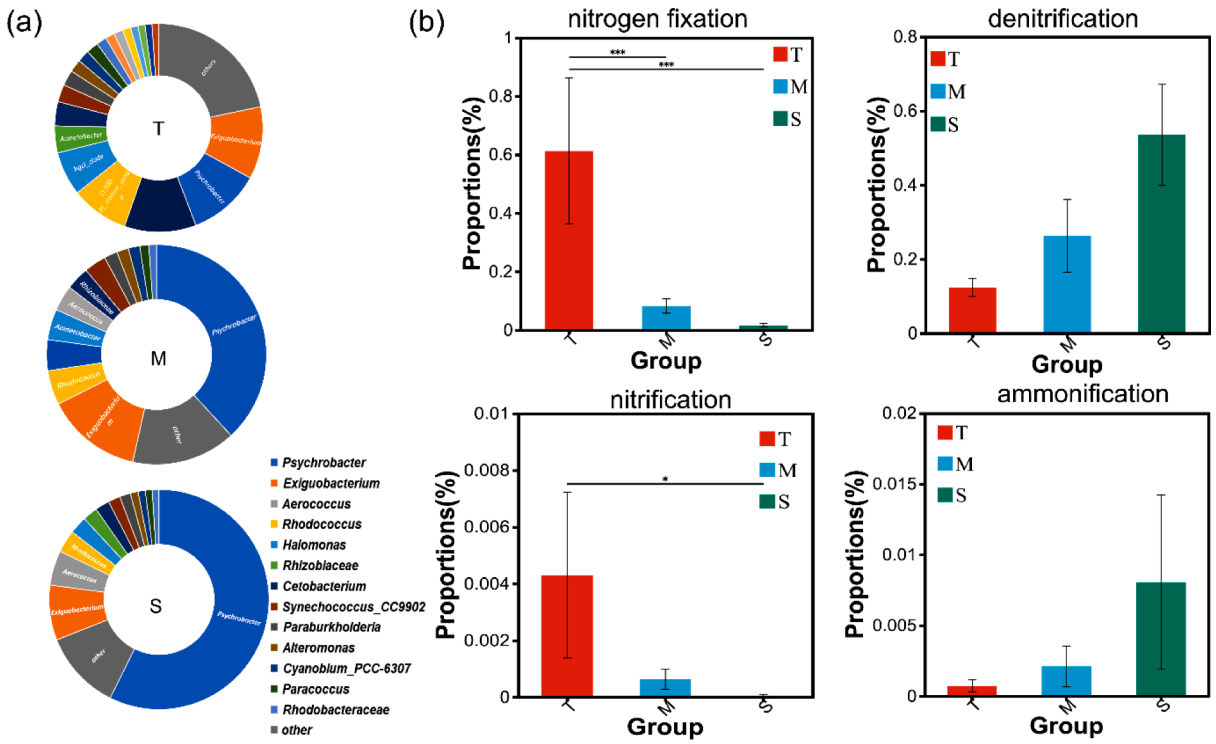

Fig. 4. Microbial structure and nitrogen functional in different regions in PRE, (a) dominant microbial species in three distinct area, (b) function heatmap of FAPROTAX function prediction in different water layer samples, and (c) comparison of dominant nitrogen transformation function in T, M and S area.

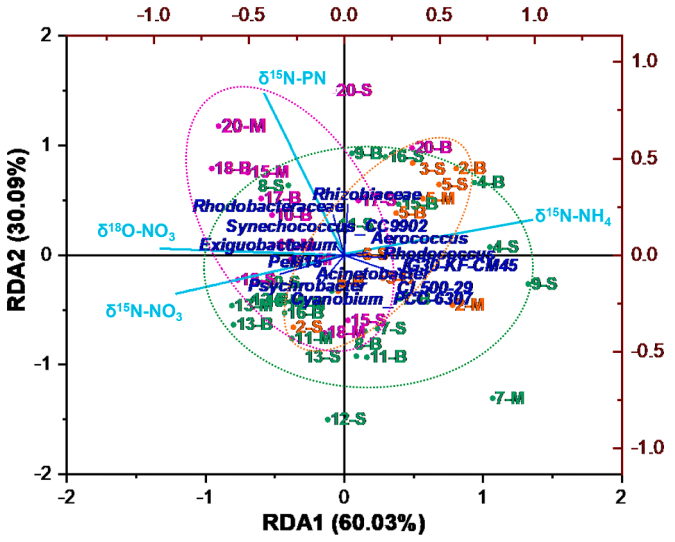

Fig. 5. RDA analysis of microbial communities (OUT level) and nitrogen isotopes. Orange labeled dots are sites in the T area, green labeled dots correspond to sites in the M area, while purple ones in the S area; The orange dashed circle is cluster in terrestrial area, green circle in mixing area, and purple one in S area. All circles are clustered within a 95 % confidence range.

ammonium (Table S1). Nitrate levels in estuaries have elevated due to increased human activities such as sewage discharge, agriculture, and industry over the past few decades (Tanaka et al., 2021). Therefore, it is prior to interpreting the nitrate fate in PRE. In general, nitrate in estuaries could be classified into source and sink processes. Our analysis of $\delta^{15}N$–NO_3^- isotopes revealed that sewage from surrounding coastal regions, particularly from mega cities like Guangzhou (GZ), Dongguan (DG), Shenzhen (SZ) and Hongkong (HK) (Fig. S2), was the primary source of NO_3^-in the reach of the PRE (Fig. S3(a)), which is consistent with previous research (Chen et al., 2022; Xuan et al., 2020; Ye et al., 2015). Moreover, nitrogen fixation prevails in the high nutrient area (e.g., T area) (Fig. 4b), with the main strains of nitrogen fixation (*Exiguobacterium*), which are known as potential sources for nitrate (Gouda et al., 2018). The contribution of groundwater as an important source of nitrate in estuaries has been established, as evidenced by the low nitrogen and oxygen isotopic compositions observed in inland groundwater (Wang et al., 2021). Fertilizer input in other studies may be one of the main sources in rivers (Kim et al., 2023), however, this region remains relatively a lower contribution (Fig. S5(a)). Moreover, atmospheric NO_3^- deposition, characterized by extremely high $\delta^{18}O$-NO_3^- values (>50‰) (Wu et al., 2018), likely contributes to surface waters in outer estuary (Ye et al., 2015).

In addition to external sources, the transformation between nitrogen species is also one of the sources of nitrate (Archana et al., 2018). Internal nitrification could be another contributor to the input of NO_3^- and low-$\delta^{15}N$-NO_3^- (3.38 ± 0.60‰). The distinct zones exhibit varying regressions slopes between $\delta^{15}N$ and $\delta^{18}O$, with -2.14 observed in the T zone, 2.17 in the M and 3.51 in the S zone in PRE (Figure S5(b)). These slopes far deviate from the expected assimilation slope of 1.0, suggesting the involvement of biological processes (nitrification, see in Fig. 4c) (Swart et al., 2014) or distinct nitrate sources during the transport from the upstream to the estuary. During nitrification, the isotopic composition of nitrate will change as a result of fractionation, which is the preferential removal or retention of certain isotopes (lighter isotopes) during biological or physical processes (Fig. 4a) (York et al., 2007). Nitrate concentrations have been observed to be particularly high in river outlets such as Humen. In the inner estuary, *Exiguobacterium*, which is a defined nitrifier in freshwater (Han et al., 2021) or sewage (Cui et al., 2021), dominated the microbial species, indicating the nitrification process as an important source of NO_3. Additionally, nitrification can cause decoupled variations of $\delta^{15}N$ and $\delta^{18}O$ by introducing O atoms from ambient water and DO with higher $\delta^{18}O$ values (Chen et al., 2022).

Nitrate dissipation along the salinity gradient in the PRE refers to the

decreasing nitrate concentration as water flows from the outlet to the estuary mouth at an uneven rate (Table S1). This process is influenced by a variety of factors, including hydrological conditions, nutrient availability, and microbial activity. Nitrate dissipated rapidly in the upper estuary when freshwater reaching the seawater, while in the lower estuary, nitrate reduction is less significant due to the seawater intrusion. Nitrate dissipation in the PRE is important because it affects nutrient availability, primary productivity, and other biogeochemical processes in the estuary and adjacent coastal waters. Nitrate dissipated due to simple mixing is unlikely to be the only cause of NO_3^- depletion (Fig. S3), and NO_3^- assimilation by phytoplankton growth may also be a contributing factor. Nitrate could also be removed by the denitrification process that occurs in anoxic (oxygen-depleted) water columns, where bacteria use nitrate as an electron acceptor to oxidize organic matter, ultimately producing N_2 and N_2O (Rogener et al., 2021). Specifically, during denitrification, the lighter isotopes of nitrate (e.g., $\delta^{14}N$ and $\delta^{16}O$) are preferentially removed, while the heavier isotopes (e.g., $\delta^{15}N$ and $\delta^{18}O$) are retained, resulting in an enrichment of ^{15}N in the residual nitrate pool (Fig. 5(c)). This enrichment phenomenon is evident in other findings (Fig. 2a) (Nikolenko et al., 2018). Consequently, the $\delta^{15}N$–NO_3^- and $\delta^{18}O$-NO_3^- value of the water column exhibits a conjunction increasing trend with increasing denitrification processes, especially in the S zone.

4.2. Transformation of nitrate and ammonium

Due to the synergistic influence of river discharge and coastal currents, a discernible surface salinity gradient emerges within the estuary. Salinity undergoes significant variation from the estuary's outlet to its convergence with the outer sea, influenced by the influx of runoff. Keeling plots ($\delta^{15}N$ versus 1/N) were used to distinguish between conservative mixing and biological nitrogen removal processes during the fresh-seawater exchange. A significant relationship was found between $\delta^{15}N$–NO_3^- or $\delta^{18}O$–NO_3^- and $1/NO_3^-$ in three zone ($p < 0.01$; Fig. 6(a) and (b)), except for $\delta^{18}O$–NO_3^- in the T zone, while negative linear correlation observed for the plots between $\delta^{15}N$–NO_3^- or $\delta^{18}O$–NO_3^- versus $ln(NO_3^-)$ ($p < 0.05$; Fig. 6(d) and (e)). The strong correlation between nitrogen and oxygen isotopes, as well as the reciprocal or *ln* of concentration, indicated the prevalence of NO_3^- assimilation or denitrification processes within the PRE estuary, notably in areas of elevated salinity levels. Nonetheless, based on the results of the three partitioned regions, it appears that a minor and conservative mixing of more than two end-members controlled the NO_3^- dual isotopes in the terrestrial input area. In contrast, NO_3^- assimilation or denitrification processes exhibit a higher prevalence in the mixing area and seawater area (Wei and Lin, 2021). The inner estuary was characterized by low salinity and high NO_3^- concentrations, while the outer estuary had high salinity and low NO_3^- concentrations. In the surface waters of the PRE, notably in upstream, NO_3^- levels were observed to be elevated. This finding is further supported by the significant negative correlations between *ln* (NO_3^-) and $\delta^{15}N$–NO_3^- ($p < 0.01$), as well as $\delta^{18}O$–NO_3^- (Fig. 4d and e), suggesting the occurrence of NO_3^- removal processes such as assimilation, dissimilatory nitrate reduction to ammonium (DNRA), and denitrification. In addition, the isotope enrichment factors were approximately 1.10‰ (average value) for $\delta^{15}N$–NO_3^- and 4.3‰ (average value) for $\delta^{18}O$–NO_3^- (Fig. 6(a) and (b)). The enrichment factor in this study was well below the denitrification process (enrichment factors range 10–30‰ (Dähnke et al., 2008a)), but with the range of assimilation (enrichment factors range 0.7–23‰ (Granger et al., 2004)). Therefore, assimilation are likely to be the dominant causes for the observed pattern, since both processes would lead to significant correlations between nitrate isotopic values and $ln(NO_3^-)$.

We made an intriguing observation of a significant positive correlation ($p < 0.05$) between $\delta^{15}N$–NH_4^+ and $ln(NH_4^+)$ in both three zones, particularly in the T and M area. This correlation suggests the presence of a fast NH_4^+ removal process, such as assimilation or anammox mixing area of the estuary, which may account for the non-conservative behavior of NH_4^+ in this area. Additionally, we found a significant negative correlation ($p < 0.01$) between $\delta^{15}N$-NO_3^- and $\delta^{15}N$–NH_4^+ values in both seasons (Fig. S8), implying that the occurrence of nitrification of ammonium from runoff and sewage was limited. Notably, this observation contrasts with that of urbanized rivers in PRE (Xuan et al., 2020). Therefore, it can be inferred that the nitrification process leads to

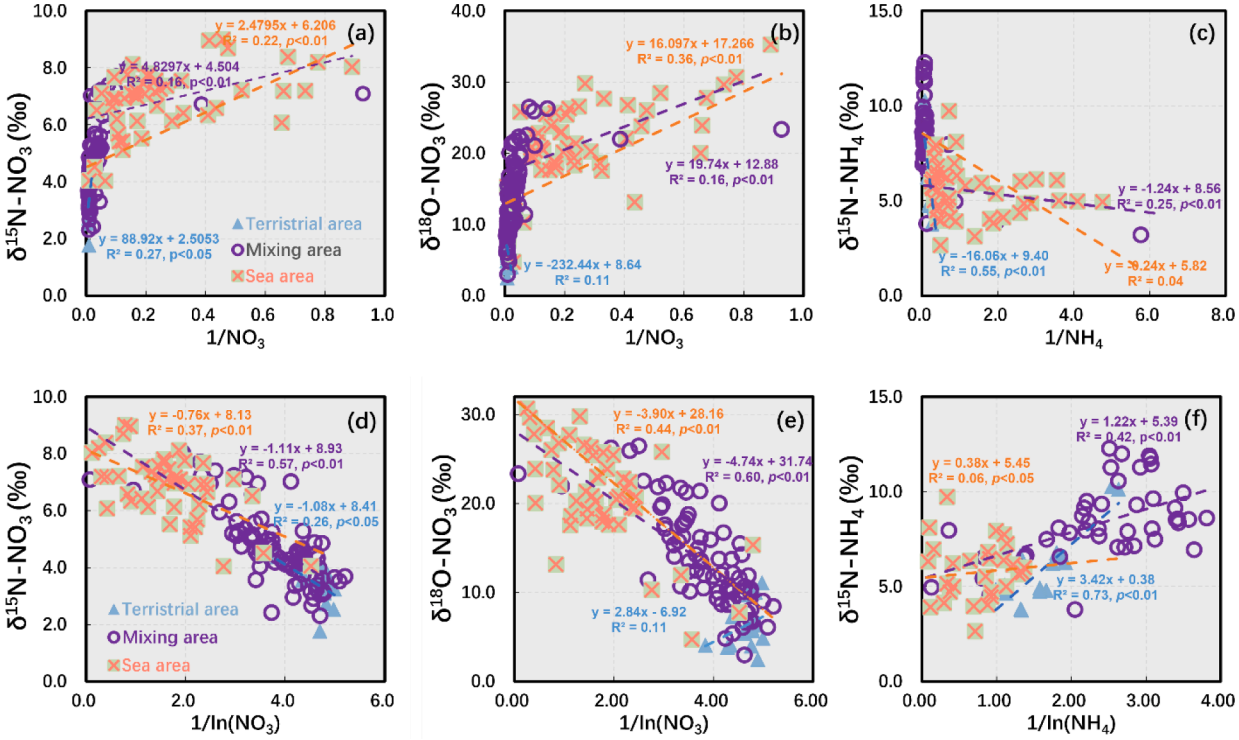

Fig. 6. Nitrate isotope variation with the reciprocal and ln of nitrate and ammonium concentration

an increase in the $\delta^{15}N–NH_4^+$ value, while the $\delta^{15}N\text{-}NO_3^-$ value decreases (Nikolenko et al., 2018). This could explain that $\delta^{15}N–NH_4^+$ values were higher in the fresh-seawater mixing area (T area) than that in the freshwater and seawater (Fig. 2 and Table S1). However, when NO_3^- is mainly derived from NH_4^+ nitrification, the $\delta^{15}N\text{-}NO_3^-$ value evolving towards the initial $\delta^{15}N–NH_4^+$ value, resulting in increased in a positive correlation between the $\delta^{15}N$ values of ammonium and nitrate (Venturi et al., 2015). Moreover, the signal of NH_4^+ assimilation, e.g., the ratio of $\delta^{15}N–NH_4^+$ with $ln(NH_4^+)$, was more obvious in the summer season (Fig. S8), which was related to (1) larger runoff discharge (including sewage, terrestrial input, and industry) with higher NH_4^+ concentrations due to the intensified rainfall scouring in summer, (2) higher assimilation rate with increased temperature and light in the summer seasons. In addition, the signal of NH_4^+ assimilation was also more obvious in the mixing area, which was characterized with relative high loads of NH_4^+. The spatial (Figure S4) and seasonal selectivity (Fig. 2) of NH_4^+ assimilation provided evidence that increase of NH_4^+ due to terrestrial input mainly from urbanization provided adequate nitrogen source and was preferentially used by phytoplankton, which caused a repression of NO_3^- removal by assimilation. Generally, nitrification results in an increase in the $\delta^{15}N$ value of NH_4^+ and a decrease in the $\delta^{15}N$ value of NO_3^- (Casciotti, 2016). NH_4^+ is considered the preferred form of nitrogen for phytoplankton uptake when both NH_4^+ and NO_3^- are available, even at low NH_4^+ concentrations ($<1\ \mu mol{\cdot}L^{-1}$), as NH_4^+ is more readily utilized than NO_3^- (Dugdale et al., 2007). Incomplete NO_3^- assimilation by phytoplankton may be responsible for elevated $\delta^{15}N\text{-}NO_3^-$ and $\delta^{18}O\text{-}NO_3^-$ values.

4.3. Assimilation of dissolved nutrients to organic particulate/plankton

In eutrophicated estuaries, runoff discharge with high nitrogen content, mainly as NO_3^- and NH_4^+, can provide ample nutrient for phytoplankton. As a result, excess nitrogen (such as NH_4^+) may stimulate phytoplankton assimilating process. NH_4^+ as the dominant process for assimilation, suppressing the removal of NO_3^- through assimilation in the PRE. The assimilation of NH_4^+ by phytoplankton can lead to an increase in the $\delta^{15}N\text{-}NH_4^+$ value (York et al., 2007), indicating this process prevailed in the mixing area (Fig. 6). The nitrogen uptake by phytoplankton preferentially assimilated light $\delta^{14}N$ rather than heavy $\delta^{15}N$ during assimilation, which could cause isotopic fractionation (Denk et al., 2017). Thus, if NO_3^- assimilation occurred, the $\delta^{15}N\text{-}PN$ was positively correlated with the $\delta^{15}N\text{-}NO_3^-$, and the $\delta^{15}N\text{-}NO_3^-$ value should be higher than the $\delta^{15}N\text{-}PN$ value. However, there was no significant correlation between $\delta^{15}N\text{-}NO_3^-$ and $\delta^{15}N\text{-}PN$ values neither in the wet season nor in the dry season (Fig. S6). In addition, the $\delta^{15}N\text{-}NO_3^-$ values of the majority samples in the wet season were lower than those of $\delta^{15}N\text{-}PN$, indicating that it seems unlikely that NO_3^- uptake by assimilation of phytoplankton. On the contrary, a significant correlation

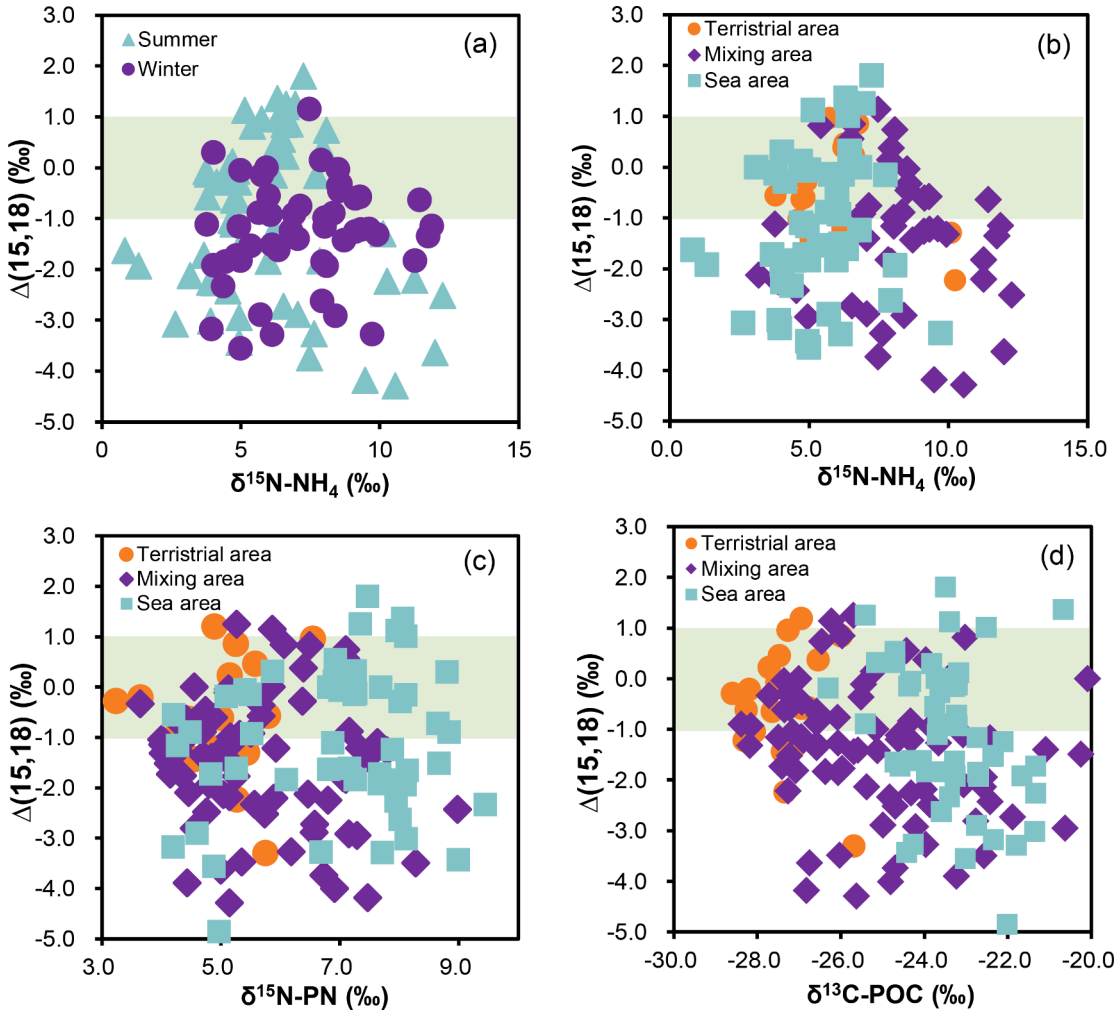

Fig. 7. Coupling variations of Δ(15,18) with $\delta^{13}C$-POC and $\delta^{15}N$-PN along the upstream to the downstream in different seasons and areas. (a) Δ(15,18) correlation with $\delta^{15}N\text{-}NO_3^-$ in summer and winter, (b) Δ(15,18) correlation with $\delta^{15}N\text{-}PN$ in different areas, (c) Δ(15,18) distribution along the $\delta^{15}N\text{-}PN$ in different areas of different areas, and (d) Δ(15,18) distribution along the $\delta^{15}N\text{-}POC$ in different areas of different area. The light green band in each panel indicates the denitrification and/or assimilation as the major NO_3^- transformation process.

between δ^{15}N-PN and δ^{15}N-NH_4^+ was observed in both wet and dry seasons (both p values lower than 0.01, Figure S5), and δ^{15}N-NH_4^+ values were higher than the δ^{15}N-PN value, indicating that assimilation occurred and phytoplankton preferred to take up NH_4^+. Overall, the isotopic evidence confirmed that uptake of NH_4^+ rather than NO_3^- was the dominant process for assimilation by phytoplankton in the PRD region, which decreased the function of assimilation in NO_3^- removal (Fig. 7). Negative correlation between δ^{15}N-PN and δ^{15}N-NH_4^+ and positive correlation of δ^{15}N-PN with δ^{15}N-NO_3^- were found in the M area (Figure S6), suggesting a phytoplankton preference for NH_4^+ uptake, potentially assimilated it into PN, while in the upstream region (T area), the lower NH_4^+ assimilation rate (Fig. 6) inhibited the NO_3^- removal process and consequently leading to elevated nitrate concentrations of the PRE.

δ^{15}N-NH_4^+ values in the summer seasons were more depleted than that in the winter seasons, attributable to the substantial contribution of NH_4^+ originating from terrestrial sources, such as domestic sewage (Xuan et al., 2020). The marine bacterium *Psychrobacter* (aquimaris A4N01) has demonstrated proficiency in establishing an effective ammonium-assimilating microbiome (Zhang et al., 2021). This bacterium efficiently removes ammonium via assimilation, a process devoid of reactive nitrogen intermediates and gaseous nitrogen emissions, as evidenced by functional gene abundance and nitrogen balance assessments. Under this circumstance, more than 80 % of ammonium, and total nitrogen are removed and recovered into biomass (Zhang et al., 2021). In the mixing area, NH_4^+ in this area was assimilated fast not only by the mean of uptake by the phytoplankton, but also the specific heterotrophic nitrifying bacteria, e.g., *Rhodococcus sp.*, in the mixed zone promoted by producing new enzyme activities and assimilating ammonium (Ma et al., 2022; Wang et al., 2022). Nitrification rate and denitrification rate of *Rhodococcus* after compound mutation had increased, thereby further enhancing the application potential of the mutant strain in the mixing area (Ma et al., 2022; Wang et al., 2022).

4.4. Nitrogen transformation process in a large-river ecosystem

Estuaries with substantial river discharge experience highly intricate elemental cycles, resulting from the combined influence of hydrological processes, biological interactions, and environmental dynamics (Cheung et al., 2021; Hitchcock et al., 2016; Wang et al., 2018; Ye et al., 2018), and act as an important source and sink of nitrogen in coastal area. In the context of the fresh-seawater mixing degree of the PRE, the projection of isotope value onto the corresponding mixing index (e.g., *q, see description in the context of the supplementary material*) reveals a quadratic regression relationship between the nitrogen isotopes of nitrate, ammonia, and particulate nitrogen and the mixing degree (Fig. 8). This observation confirms the involvement of intricate biological processes during the transport of nitrogen components from land to sea, especially during the fresh-seawater mixing. δ^{15}N-NO_3^- were univariate quadratic regressed ($y=5.41x^2-9.13x+7.20$, $p < 0.01$, Fig. 8(b)). This non-conservative mixing of nitrogen components is particularly evident in the mixing (M) zone, as indicated by the quadratic decrease of δ^{15}N-NH_4^+ (q from 1 to 0) (Fig. 8(b)) and the decline in δ^{15}N-PN (Fig. 8 (c)). These isotopic results suggest the assimilation of ammonia nitrogen into particulate nitrogen within the mixing zone. The outward path of particulate nitrogen from the mixing zone is hindered by the salinity

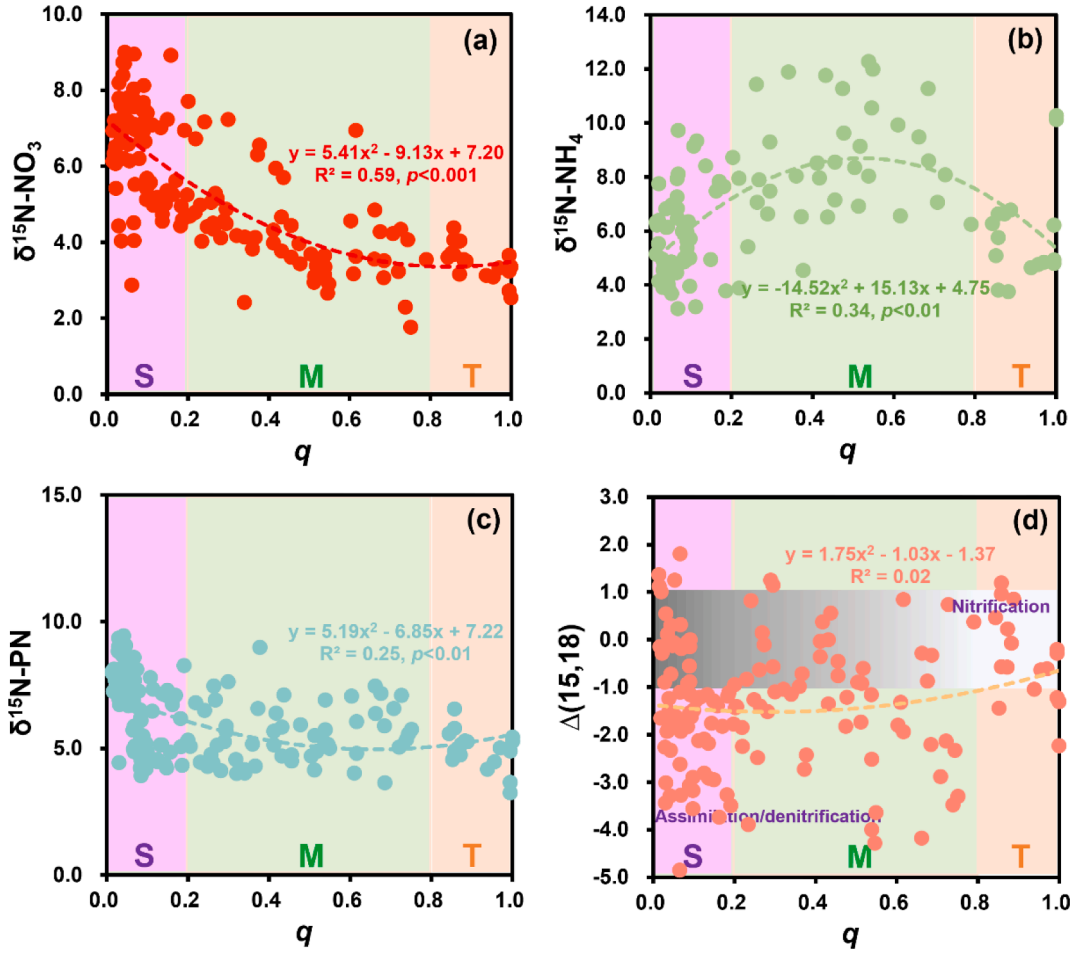

Fig. 8. Isotope variation along the degree of freshwater and seawater mixing. All data are best fitted for the quadratic regression analysis: (a) δ^{15}N-NO_3^- regression with mixing degree; (b) δ^{15}N-NH_4^+ regression with mixing degree; (c) δ^{15}N-PN regression with mixing degree; (d) Δ(15,18) regression with mixing degree.

front, and it is also affected by the assimilation of ammonia.

As reported, a remarkable portion of the total oxygen loss in the upper reach (T zone) can be attributed to nitrification-driven oxygen consumption, ranging from 28.5 % to 44.1 % (Jiang et al., 2021). In the T zone characterized by low salinity and high turbidity, nitrogen assimilation is inhibited, leading to constrained primary productivity (Howarth and Marino, 2006; Middelbo et al., 2018). In the inner estuary, the predominant bacterial population, specifically *Exiguobacterium sp.*, assumes responsibility for the process of nitrification (Cui et al., 2021). The higher concentration of suspended particulate matter can facilitate the proliferation of nitrifying microorganisms, including *Exiguobacterium* sp. (Cui et al., 2021). The downstream area of the estuary demonstrated insignificant effects of nitrification on oxygen depletion. One explanation for this phenomenon is the preferential association of the majority of microorganisms responsible for ammonia oxidation, namely ammonia-oxidizing bacteria and ammonia-oxidizing archaea, with particulate matter in estuarine environments (Wei and Lin, 2021; Zheng et al., 2014). The decomposition of suspended organic matter can contribute to the generation of ammonium, subsequently triggering nitrification (Zhang et al., 2023). However, it has been hypothesized that prolonged water residence times are necessary to facilitate the proliferation of slow-growing bacterial populations, which play a crucial role in the nitrification of available ammonium (Dai et al., 2008). This scenario is more likely to occur under conditions of reduced flow in the inner or eastern PRE (Mao et al., 2004; Wong et al., 2003). Due to the substantial input of terrestrial matter and the intricate biological activities observed in estuaries, including the priming effects of newly produced nitrogen during the fresh-seawater mixing and the rich plankton biodiversity in high-salinity regions (Dähnke et al., 2008b; Jiang et al., 2021), the nitrogen transformation process exhibits high variability and complexity. These findings provide substantial evidence regarding the multi-isotope dynamics.

Upon entering the estuary, nitrogen is trapped within the mixing zone owing to the intrusion of seawater, thereby fostering eutrophication. Therefore, profound comprehension of the nitrogen transformation dynamics during the fresh-seawater mixing is instrumental in grasping and mitigating nitrogen pollution within the mixing zone. Moreover, it expedites the dilution of nitrogen within the estuary, ultimately influencing the nitrogen quality in this region, which helps in governing the nitrogen pollution in estuaries. This research demonstrates a clear and comprehensive characterization of the nitrogen transformation process in an anthropogenic dominated estuary, highlighting its importance for regulating the nitrogen dissipation in the fresh-seawater mixing process in estuarine ecosystems.

5. Conclusions

Our study reveals key insights into nitrogen dynamics within the estuaries of large coastal rivers during the fresh-seawater mixing processes. NO_3^- and NH_4^+ originating from domestic sewage and groundwater discharge elevated and dominated in the inner estuary. The contribution from anthropogenic sources of nitrate were under a relatively higher nitrogen fixation and nitrification rate, primarily driven by *Exiguobacterium sp*. And this process was more pronounced in the estuarine outlets compared to the fresh-seawater mixing zones. In contrast, outside the estuary (S area), atmospheric deposition plays a substantial source in seawater nitrate, while NH_4^+ arising from NO_3^- ammonification. This process leads to the transformation of dissolved to particulate nitrogen. Moreover, denitrification processes are dominant in the S area, as evidenced by elevated δ^{15}N- NO_3^- isotopes and microbial functional results. The intricate nitrogen transformation process occurs in the fresh-seawater area in PRE. Here, NO_3^- and NH_4^+ rapidly diluted when freshwater research the seawater. Moreover, higher δ^{15}N-NH_4^+ values indicated that NH_4^+ assimilated by phytoplankton/bacteria, such as *Psychrobacter sp.* and *Rhodococcus*, in the M area, which turns the NH_4^+ into PN. These findings provide valuable insights into the transport and transformation of nitrogen in estuarine environments, laying the groundwork for addressing the detrimental effects of excessive anthropogenic nitrogen inputs. Our research contributes novel perspectives to nitrogen management in estuarine ecosystems, particularly in regions characterized by freshwater-seawater mixing processes.

Declaration of Competing Interest

The authors declare that they have no known competing financial interests or personal relationships that could have appeared to influence the work reported in this paper.

Data availability

Data will be made available on request.

Acknowledgment

This research was supported by Grants from the National Natural Science Foundation of China (NSFC, 41890852, 41906133, and U1901221), the Key Special Project for Introduced Talents Team of the Southern Marine Science and Engineering Guangdong Laboratory (Guangzhou) (GML2019ZD0405). This work was also supported by the Science and Technology Planning Project of Guangdong Province, China (2023B1212060047).

Supplementary materials

Supplementary material associated with this article can be found, in the online version, at doi:10.1016/j.watres.2023.120809.

References

Adyasari, D., Hassenrück, C., Montiel, D., Dimova, N., 2020. Microbial community composition across a coastal hydrological system affected by submarine groundwater discharge (SGD). PLoS One 15, e0235235.
Archana, A., Thibodeau, B., Geeraert, N., Xu, M.N., Kao, S.J., Baker, DM., 2018. Nitrogen sources and cycling revealed by dual isotopes of nitrate in a complex urbanized environment. Water Res. 142, 459–470.
Böhlke, J.K., Mroczkowski, S.J., Coplen, TB., 2003. Oxygen isotopes in nitrate: new reference materials for ^{18}O:^{17}O:^{16}O measurements and observations on nitrate-water equilibration. Rapid Commun. Mass Spectrom. 17, 1835–1846.
Bruesewitz, D.A., Gardner, W.S., Mooney, R.F., Pollard, L., Buskey, EJ., 2013. Estuarine ecosystem function response to flood and drought in a shallow, semiarid estuary: nitrogen cycling and ecosystem metabolism. Limnol. Oceanogr. 58, 2293–2309.
Casciotti, KL., 2016. Nitrite isotopes as tracers of marine N cycle processes. Philos. Trans. R. Soc. Math. Phys. Eng. Sci. 374, 20150295.
Chen, F., Deng, Z., Lao, Q., Bian, P., Jin, G., Zhu, Q., et al., 2022. Nitrogen cycling across a salinity gradient from the Pearl River Estuary to offshore: insight from nitrate dual isotopes. J. Geogr. Res. Biogeosciences 127, e2022JG006862.
Chen, R.R., Dittert, K., 2008. Diffusion technique for 15N and inorganic N analysis of low-N aqueous solutions and Kjeldahl digests. Rapid Commun. Mass Spectrom. 22, 1727–1734.
Cheung, Y.Y., Cheung, S., Mak, J., Liu, K., Xia, X., Zhang, X., et al., 2021. Distinct interaction effects of warming and anthropogenic input on diatoms and dinoflagellates in an urbanized estuarine ecosystem. Glob. Change Biol. 27, 3463–3473.
Cui, Y., Cui, Y.W., Huang, J-L., 2021. A novel halophilic Exiguobacterium mexicanum strain removes nitrogen from saline wastewater via heterotrophic nitrification and aerobic denitrification. Bioresour. Technol. 333, 125189.
Dähnke, K., Bahlmann, E., Emeis, K., 2008a. A nitrate sink in estuaries? An assessment by means of stable nitrate isotopes in the Elbe estuary. Limnol. Oceanogr. 53, 1504–1511.
Dähnke, K., Bahlmann, E., Emeis, K., 2008b. A nitrate sink in estuaries? An assessment by means of stable nitrate isotopes in the Elbe estuary. Limnol. Oceanogr. 53, 1504–1511.
Dai, M., Wang, L., Guo, X., Zhai, W., Li, Q., He, B., et al., 2008. Nitrification and inorganic nitrogen distribution in a large perturbed river/estuarine system: the Pearl River Estuary, China. Biogeosciences 5, 1227–1244.
Denk, T.R.A., Mohn, J., Decock, C., Lewicka-Szczebak, D., Harris, E., Butterbach-Bahl, K., et al., 2017. The nitrogen cycle: A review of isotope effects and isotope modeling approaches. Soil Biol. Biochem. 105, 121–137.
Diaz, R.J., Rosenberg, R., 2008. Spreading dead zones and consequences for marine ecosystems. Science 321, 926–929.

Dugdale, R.C., Wilkerson, F.P., Hogue, V.E., Marchi, A., 2007. The role of ammonium and nitrate in spring bloom development in San Francisco Bay. Estuarine Coastal Shelf Sci. 73, 17–29.
Gouda, S., Kerry, R.G., Das, G., Paramithiotis, S., Shin, H.S., Patra, J.K., 2018. Revitalization of plant growth promoting rhizobacteria for sustainable development in agriculture. Microbiol. Res. 206, 131–140.
Granger, J., Sigman, D.M., Needoba, J.A., Harrison, P.J., 2004. Coupled nitrogen and oxygen isotope fractionation of nitrate during assimilation by cultures of marine phytoplankton. Limnol. Oceanogr. 49, 1763–1773.
Gruber, N., Capone, D.G., Bronk, D.A., Mulholland, M.R., Carpenter, E.J., 2008. Chapter 1 - The marine nitrogen cycle: overview and challenges. Nitrogen in the Marine Environment, Second Ed. Academic Press, San Diego, pp. 1–50.
Han, X., Qu, Y., Dong, Y., Chen, D., Liang, D., Liu, J., et al., 2021. Simultaneous electricity generation and eutrophic water treatment utilizing iron coagulation cell with nitrification and denitrification biocathodes. Sci. Total Environ. 782, 146436.
Hitchcock, J.N., Mitrovic, S.M., Hadwen, W.L., Roelke, D.L., Growns, I.O., Rohlfs, AM., 2016. Terrestrial dissolved organic carbon subsidizes estuarine zooplankton: an *in situ* mesocosm study. Limnol. Oceanogr. 61, 254–267.
Hodoki, Y., Ohbayashi, K., Tanaka, N., Kunii, H., 2013. Evaluation of genetic diversity in zostera japonica (Aschers. et Graebn.) for Seagrass conservation in brackish lower reaches of the hii river system, Japan. Estuaries Coasts 36, 127–134.
Howarth, R.W., Marino, R., 2006. Nitrogen as the limiting nutrient for eutrophication in coastal marine ecosystems: Evolving views over three decades. Limnol. Oceanogr. 51, 364–376.
Jiang, H., Ma, J., Xu, H., Xu, Z.F., Liu, W.J., Pan, K., 2021. Multiple isotopic compositions reveal complex nitrogen cycling in a subtropical estuary. Environ. Pollut. 272.
Karthäuser, C., Ahmerkamp, S., Marchant, H.K., Bristow, L.A., Hauss, H., Iversen, M.H., et al., 2021. Small sinking particles control anammox rates in the Peruvian oxygen minimum zone. Nat. Commun. 12, 3235.
Keats, R.A., Osher, L.J., Neckles, HA., 2004. The effect of nitrogen loading on a brackish estuarine faunal community: A stable isotope approach. Estuaries 27, 460–471.
Kendall, C., Silva, S.R., Kelly, VJ., 2001. Carbon and nitrogen isotopic compositions of particulate organic matter in four large river systems across the United States. Hydrol. Processes 15, 1301–1346.
Kim, S.H., Lee, D., Kim, M.S., RH, H.J., Shin, K.H., 2023. Systematic tracing of nitrate sources in a complex river catchment: An integrated approach using stable isotopes and hydrological models. Water Res., 119755
Lin, J., Krom, M.D., Wang, F., Cheng, P., Yu, Q., Chen, N., 2022. Simultaneous observations revealed the non-steady state effects of a tropical storm on the export of particles and inorganic nitrogen through a river-estuary continuum. J. Hydrol. 606, 127438.
Loken, L.C., Small, G.E., Finlay, J.C., Sterner, R.W., Stanley, EH., 2016. Nitrogen cycling in a freshwater estuary. Biogeochemistry 127, 199–216.
Ma, S., Huang, S., Tian, Y., Lu, X., 2022. Heterotrophic ammonium assimilation: an important driving force for aerobic denitrification of Rhodococcus erythropolis strain Y10. Chemosphere 291, 132910.
Mao, Q., Shi, P., Yin, K., Gan, J., Qi, Y., 2004. Tides and tidal currents in the Pearl River Estuary. Cont. Shelf Res. 24, 1797–1808.
McLaughlin, K., Nezlin, N.P., Howard, M.D.A., Beck, C.D.A., Kudela, R.M., Mengel, M.J., et al., 2017. Rapid nitrification of wastewater ammonium near coastal ocean outfalls, Southern California, USA. Estuarine Coastal Shelf Sci. 186, 263–275.
Middelbo, A.B., Sejr, M.K., Arendt, K.E., Møller, EF., 2018. Impact of glacial meltwater on spatiotemporal distribution of copepods and their grazing impact in Young Sound NE, 63. Greenland, pp. 322–336.
Nikolenko, O., Jurado, A., Borges, A.V., Knöller, K., Brouyère, S., 2018. Isotopic composition of nitrogen species in groundwater under agricultural areas: A review. Sci. Total Environ. 621, 1415–1432.
Rogener, M.K., Hunter, K.S., Rabalais, N.N., Roberts, B.J., Bracco, A., Stewart, F.J., et al., 2021. Pelagic denitrification and methane oxidation in oxygen-depleted waters of the Louisiana shelf. Biogeochemistry 154, 231–254.
Schlesinger, WH., 2009. On the fate of anthropogenic nitrogen. Proc. Natl Acad. Sci. 106, 203–208.
Seitzinger, S.P., Kroeze, C., Bouwman, A.F., Caraco, N., Dentener, F., Styles, RV., 2002. Global patterns of dissolved inorganic and particulate nitrogen inputs to coastal systems: Recent conditions and future projections. Estuaries 25, 640–655.
Sigman, D.M., Casciotti, K.L., Andreani, M., Barford, C., Galanter, M., Bohlke, JK., 2001. A bacterial method for the nitrogen isotopic analysis of nitrate in seawater and freshwater. Anal. Chem. 73, 4145–4153.
Sigman, D.M., Granger, J., DiFiore, P.J., Lehmann, M.M., Ho, R., Cane, G., et al., 2005. Coupled nitrogen and oxygen isotope measurements of nitrate along the eastern North Pacific margin. Glob. Biogeochem. Cycles 19, GB4022.
Sinha, E., Michalak, A.M., Balaji, V., 2017. Eutrophication will increase during the 21st century as a result of precipitation changes. Science 357, 405–408.
IdC, S., HP, A., Azevedo, V.C., Duarte, I.D., Rocha, L.D., Matsumoto, S.T., et al., 2021. Different trophodynamics between two proximate estuaries with differing degrees of pollution. Sci. Total Environ. 770, 144651.
Swart, P.K., Evans, S., Capo, T., Altabet, MA., 2014. The fractionation of nitrogen and oxygen isotopes in macroalgae during the assimilation of nitrate. Biogeosciences 11, 6147–6157.
Tanaka, Y., Minggat, E., Roseli, W., 2021. The impact of tropical land-use change on downstream riverine and estuarine water properties and biogeochemical cycles: a review. Ecol. Process. 10, 40.
Venturi, S., Vaselli, O., Tassi, F., Nisi, B., Pennisi, M., Cabassi, J., et al., 2015. Geochemical and isotopic evidences for a severe anthropogenic boron contamination: A case study from Castelluccio (Arezzo, central Italy). Appl. Geochem. 63, 146–157.
Wang, C., Lv, Y., Li, Y., 2018. Riverine input of organic carbon and nitrogen in water-sediment system from the Yellow River estuary reach to the coastal zone of Bohai Sea. China. Continental Shelf Res. 157, 1–9.
Wang, J., Chen, P., Li, S., Zheng, X., Zhang, C., Zhao, W., 2022. Mutagenesis of high-efficiency heterotrophic nitrifying-aerobic denitrifying bacterium Rhodococcus sp. strain CPZ 24. Bioresour. Technol. 361, 127692.
Wang, X., Zhang, Y., Luo, M., Xiao, K., Wang, Q., Tian, Y., et al., 2021. Radium and nitrogen isotopes tracing fluxes and sources of submarine groundwater discharge driven nitrate in an urbanized coastal area. Sci. Total Environ. 763, 144616.
Wei, H., Lin, X., 2021. Shifts in the relative abundance and potential rates of sediment ammonia-oxidizing archaea and bacteria along environmental gradients of an urban river–estuary–adjacent sea continuum. Sci. Total Environ. 771, 144824.
Wong, L.A., Chen, J.C., Xue, H., Dong, L.X., Su, J.L., Heinke, G., 2003. A model study of the circulation in the Pearl River Estuary (PRE) and its adjacent coastal waters: 1. Simulations and comparison with observations. J. Geogr. Res. Oceans 108.
Wong, W.W., Pottage, J., Warry, F.Y., Reich, P., Roberts, K.L., Grace, M.R., et al., 2018. Stable isotopes of nitrate reveal different nitrogen processing mechanisms in streams across a land use gradient during wet and dry periods. Biogeosciences 15, 3953–3965.
Wu, Y., Zhang, J., Liu, S., Jiang, Z., Arbi, I., Huang, X., et al., 2018. Nitrogen deposition in precipitation to a monsoon-affected eutrophic embayment: Fluxes, sources, and processes. Atmos. Environ. 182, 75–86.
Xuan, Y., Tang, C., Cao, Y., 2020. Mechanisms of nitrate accumulation in highly urbanized rivers: Evidence from multi-isotopes in the Pearl River Delta, China. J. Hydrol. 587, 124924.
Ye, F., Guo, W., Wei, G., Jia, G., 2018. The sources and transformations of dissolved organic matter in the Pearl River Estuary, China, as revealed by stable isotopes. J. Geogr. Res. Oceans 123, 6893–6908.
Ye, F., Jia, G., Wei, G., Guo, W., 2022. A multi-stable isotopic constraint on water column oxygen sinks in the Pearl River Estuary, South China. Mar. Environ. Res., 105643
Ye, F., Ni, Z., Xie, L., Wei, G., Jia, G., 2015. Isotopic evidence for the turnover of biological reactive nitrogen in the Pearl River Estuary, south China. J. Geogr. Res. Oceans 120, 661–672.
York, J.K., Tomasky, G., Valiela, I., Repeta, DJ., 2007. Stable isotopic detection of ammonium and nitrate assimilation by phytoplankton in the Waquoit Bay estuarine system. Limnol. Oceanogr. 52, 144–155.
Zhang, L., Chen, M., Zheng, Y., Wang, J., Xiao, X., Chen, X., et al., 2023. Microbially driven fate of terrigenous particulate organic matter in oceans. Limnol. Oceanogr. 68, 148–164.
Zhang, M., Han, F., Li, Y., Liu, Z., Chen, H., Li, Z., et al., 2021. Nitrogen recovery by a halophilic ammonium-assimilating microbiome: A new strategy for saline wastewater treatment. Water Res. 207, 117832.
Zhang, M., Han, F., Liu, Z., Han, Y., Li, Y., Zhou, W., 2022. Ammonium-assimilating microbiome: A halophilic biosystem rationally optimized by carbon to nitrogen ratios with stable nitrogen conversion and microbial structure. Bioresour. Technol. 350, 126911.
Zheng, Y., Hou, L., Newell, S., Liu, M., Zhou, J., Zhao, H., et al., 2014. Community dynamics and activity of ammonia-oxidizing prokaryotes in intertidal sediments of the yangtze estuary. Appl. Environ. Microbiol. 80, 408–419.
Zhu, A., Chen, J., Gao, L., Shimizu, Y., Liang, D., Yi, M., et al., 2019. Combined microbial and isotopic signature approach to identify nitrate sources and transformation processes in groundwater. Chemosphere 228, 721–734.